Applied Physics Letters ARTICLE scitation.org/journal/apl

Rapid absolute sizing of deeply subwavelength dielectric nanoparticles by confocal scanning optical microscopy

Cite as: Appl. Phys. Lett. **118**, 241105 (2021); doi: 10.1063/5.0057471
Submitted: 21 May 2021 · Accepted: 22 May 2021 ·
Published Online: 16 June 2021

Swetapadma Sahoo, Hana Azzouz, and Simeon I. Bogdanov[a)]

AFFILIATIONS

Department of Electrical and Computer Engineering, University of Illinois at Urbana-Champaign, Urbana, Illinois 61801, USA and Holonyak Micro and Nanotechnology Lab, University of Illinois at Urbana-Champaign, Urbana, Illinois 61801, USA

[a)]Author to whom correspondence should be addressed: bogdanov@illinois.edu

ABSTRACT

Accurate sizing of individual nanoparticles is crucial for the understanding of their physical and chemical properties and for their use in nanoscale devices. Optical sizing methods are non-invasive, rapid, and versatile. However, the low optical response of weakly absorbing subwavelength dielectric nanoparticles poses a fundamental challenge for their optical metrology. We demonstrate scalable optical sizing of such nanoparticles based on confocal scanning microscopy. The method is absolutely calibrated by correlating the optical signatures in the scattered pump laser signal to the ground truth nanoparticle sizes measured by an atomic force microscope. Using an air objective with a numerical aperture of 0.9, we measured the sizes of nanodiamond particles ranging from 35 to 175 nm, with an average error of ± 12.7 nm compared to the ground truth sizes. This technique paves the way for the metrology of a wide range of weakly scattering nano-objects for applications in biomedicine, catalysis, nanotechnology, and quantum optics.

With rapid advances in nanotechnology, the detection and metrology of individual nanoparticles have become crucial for a wide range of applications, ranging from biosensing[1] to quantum optical devices.[2] The most sensitive techniques for the sizing of individual nanoparticles include atomic force microscopy (AFM), transmission electron microscopy (TEM), and scanning electron microscopy (SEM). AFM characterization yields precise height measurement of nanoparticles on flat substrates, down to a single nanometer, but is limited by the slow scanning speeds required for such accuracy.[3] Electron microscopy techniques provide excellent lateral resolution but require special sample preparation and introduce carbon contamination[4] and charges.[5] Optical sizing methods are non-invasive, feature high throughput,[6] and are directly compatible with a variety of other optical measurements such as those of Raman scattering,[7] fluorescence,[8] or parametric response.[9]

However, optical sizing methods are spatially limited by the wavelength of light. Their applicability strongly depends on the size and optical properties of nanoparticles. The metrology of subwavelength metallic nanoparticles, down to a few nanometers, is facilitated by the presence of localized surface plasmon resonances.[10–12] As for dielectric nanoparticles, inferring their individual sizes by optical scattering techniques[13–17] has so far been challenging in the sub-100 nm range, particularly for weakly absorbing materials. The scattering cross section in dielectric particles scales as the volume squared in the Rayleigh limit, while absorption scales proportionally to the nanoparticle volume.[18] The sizing of weakly absorbing nanoparticles must rely on their vanishingly small scattering signals. Sizing of such particles has been possible using whispering gallery resonators[19] and laser cavity spectrometers.[20] However, these characterization techniques based on high quality factor resonances require co-locating the particle with the resonator as well as tuning the excitation in resonance with the optical mode. Other recently reported techniques rely on photonic crystals[21] and plasmonic resonances[22] on specially patterned substrates. These requirements limit the practicality of resonance-based techniques.

Here, we use a confocal microscopy setup to acquire scattered light signatures from inhomogenously sized nanodiamonds (NDs). After the initial calibration of the instrument using ground truth particle height measurements obtained by AFM, we are able to predict ND sizes through optical scattering signatures. Using an air objective, we demonstrate sizing of individual NDs down to a diameter of ∼35 nm, much below the range of sizes that exhibit optical resonances in the

visible spectrum.[23] Our approach provides an accessible method for the sizing of individual weakly absorbing subwavelength nano-objects.

Our sample consisted of NDs (Adamas Nano NDNV100 nm) randomly dispersed on a 170 μm thick glass coverslip substrate. A CW green laser (Coherent OBIS 520LX) operating at $\lambda_0 = 520$ nm with an incident intensity of 4 mW, spatially filtered by a pinhole, was used to pump the sample's top surface containing the NDs through an NA = 0.9 air objective (Nikon MUE12900). We used a home-built scanning confocal microscope to acquire scattering maps of 54 NDs (Fig. 1). The objective scanning was performed by a three-axis piezoelectric stage (P-561, Physik Instrumente) with a range of 100 μm and a resolution of 0.8 nm. The pump light reflected by the sample was collected and collimated by the same objective, separated from the incident pump by a beam splitter, and focused into an avalanche photodiode (Hamamatsu C10508-01) through a confocal pinhole. During the scan, the smooth coverslip surface yielded a constant reflection signal. As the laser beam waist was scanned over an ND, the scattering by the nanoparticle modified the reflected signal, producing characteristic dark features on the acquired maps [Fig. 2(a)].

We determined the "ground truth" heights of the same NDs by acquiring 1 μm × 1 μm sized "headshots" using a high-resolution AFM (Asylum Cypher S). Figure 2(b) features several representative AFM headshots for NDs of different sizes. Finally, we also show the widefield camera images of the NDs in Fig. 2(c) acquired by illuminating the sample with a broadband lamp. Each row of images in Fig. 2 corresponds to a specific ND. We note that for ND heights below 80 nm, the particles do not appear on the widefield camera images but produce measurable reflection dips on the confocal scans. This is indicative of the extended dynamic range of confocal imaging, compared to widefield imaging, for the sizing of dielectric nanoparticles.

From Figs. 2(a) and 2(b), a positive correlation between the size of confocal map features and the AFM-measured sizes of nanodiamonds can be inferred. We now show that these optical features can indeed be used as a measure of ND size by confronting them with the ground truth measurements. To quantify the size-related information obtained from confocal reflection maps, we define an area parameter A_i corresponding to every individual reflection feature (see Fig. 3). First, the scattered light intensity was normalized by the reflected intensity from a flat sample area on the coverslip. The scattering features of NDs exhibited distinctively lower intensity values than the flat glass substrate areas did. Next, for each reflection feature, we counted the number of pixels N_i with intensities below a threshold. The threshold was taken at the lower end of the intensity histogram formed by pixels belonging to a flat area surrounding the ND (background pixels). We converted N_i into an area A_i, knowing the physical size of the confocal map pixel of 50 nm. Figure 3(a) shows a characteristic reflection feature from a nanodiamond with ground truth height of $h = 83$ nm. In Fig. 3(b), we show a cross section of the reflection intensity profile along the blue line passing through the ND. The ensemble of pixels below the threshold value defines the area A.

Diamonds with $h > 35$ nm yielded discernible features in the confocal reflection intensity profiles, from which the area A could be

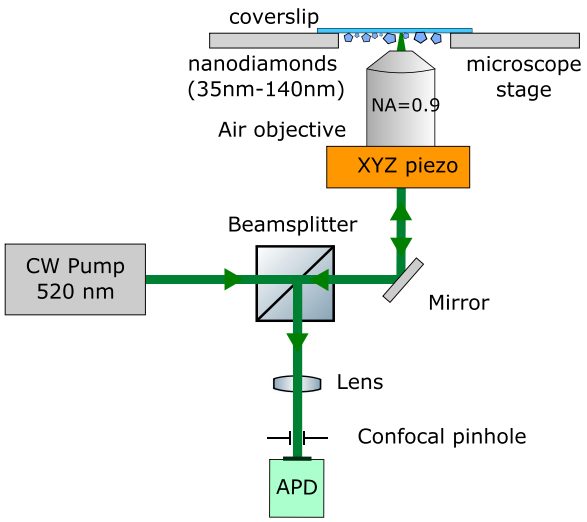

FIG. 1. Schematic of the confocal scanning setup. A 520 nm pump laser illuminates the sample with randomly dispersed NDs. The objective with NA = 0.9 is scanned by a 3-axis piezo stage. The reflected light is collected to produce a scanning image of the nanodiamonds using an avalanche photodiode (APD).

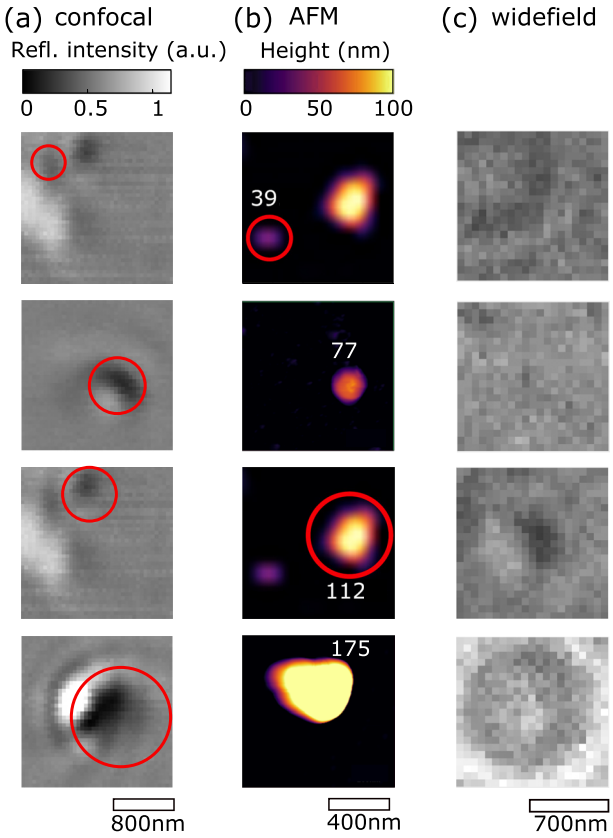

FIG. 2. Size-related data for representative individual NDs used in the study. (a) 2 μm confocal pump reflection scans with a pixel size of 25 nm. For each row, red circles indicate the features corresponding to the same NDs (b) 1 μm AFM height scans (c) widefield 1.3 μm by 1.3 μm camera images of the same areas as in (a) and (b). Single NDs with height below ~77 nm produce distinct features on the confocal scans but do not appear on the widefield images.

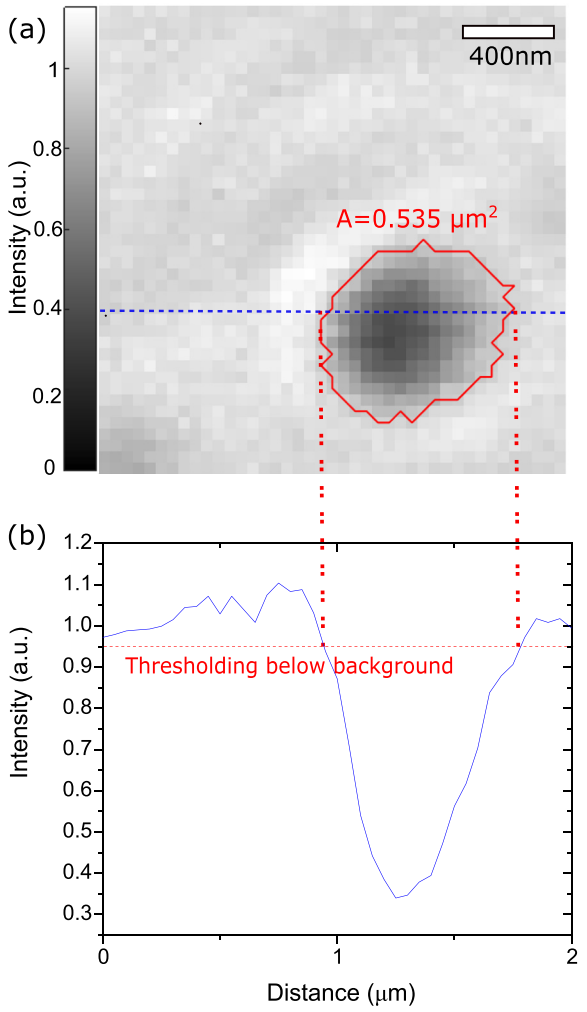

FIG. 3. Quantification of the confocal reflection intensity profile for an ND with AFM-measured height $h = 83$ nm. (a) The ND location is associated with a characteristic dip in the confocally detected reflection intensity due to scattering by the nanoparticle. The reflected intensity in the map is normalized by the intensity measured from a flat coverslip area. The area A is defined as the total area of all the pixels in the connected reflection feature with an intensity less than the threshold determined from background. Here, our area parameter $A = 0.535$ μm^2 is formed by 214 pixels with a size of 50 nm. (b) Reflection intensity profile along the blue line in (a) normalized by the average background level.

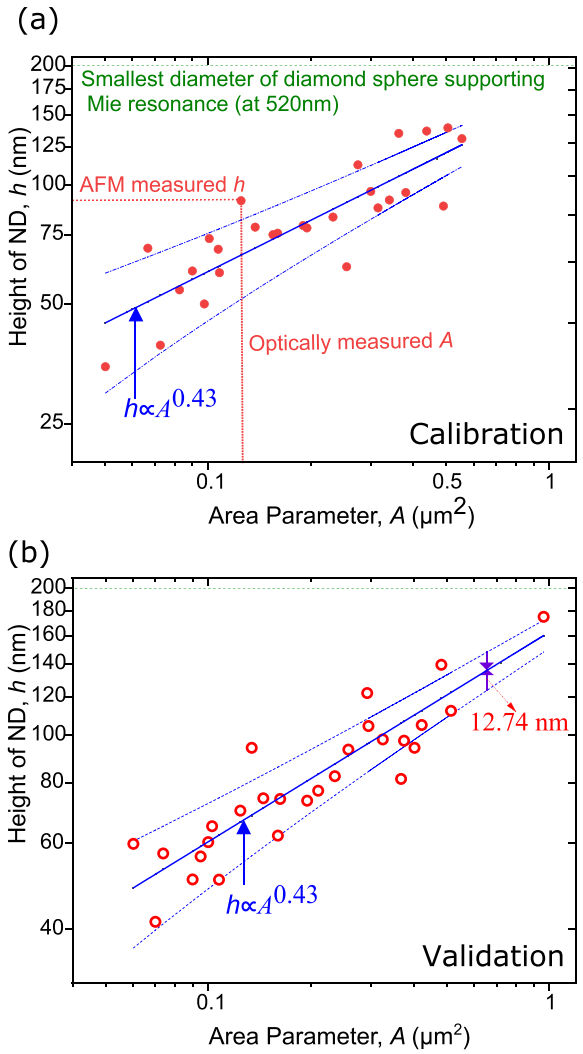

FIG. 4. The ground truth ND heights measured by AFM plotted against the area parameters A determined from confocal reflection intensity maps. (a) The data of the calibration set is fit by a power law, represented by the solid blue line. The dashed bands represent the accuracy of the confocal sizing method. (b) The correlation obtained from (a) is verified with a second dataset, yielding an accuracy of ± 12.7 nm. Each ND has a size well below the minimal diameter $d_0 \approx 200$ nm necessary for a diamond sphere to sustain a Mie resonance at $\lambda_0 = 520$ nm in vacuum.

extracted. The h_i in our dataset ranged from 35 to 140 nm or from $0.07\lambda_0$ to $0.27\lambda_0$. In particular, these sizes are well below the diameter d_0 of the smallest diamond sphere supporting a Mie resonance in vacuum.

We divide all the NDs in our dataset into two groups of 27 NDs each, forming a calibration and validation set. For all the NDs in the calibration set, we fit the dependence $h(A)$ with a power law, extracting an exponent value of 0.43 [Fig. 4(a)]. The extracted trendline $h = kA^{0.43}$ can now be used to "predict" the sizes of NDs from the validation set. We assess the accuracy of our optical nanoparticle sizing method on the validation set by calculating the average difference between the ground truth sizes and the "predicted" values given by the trend line [Fig. 4(b)]. This accuracy is given by $\sigma = \sqrt{\langle (h_i - kA_i^{0.43})^2 \rangle_{\text{val}}} = \pm 12.7$ nm for the validation set, quantifying the performance of confocal microscopy as an absolute sizing method for dielectric nanoparticles. In this study, we do not consider the influence of possible ND particle asymmetries on the confocal reflection intensity profiles. Therefore, part of this accuracy value is expected to be caused by the natural dispersion in nanodiamond aspect ratios.[24]

Accurate optical nanoparticle sizing through confocal microscopy has wide applications across several fields. It is directly

compatible with the optical characterization of functional nanoparticles, offering a rapid pre-selection tool for the deterministic assembly of nanoparticle-based quantum photonic[25,26] and semiconductor devices.[27,28] The method can assist in targeting, tracking, and studying size-dependent degradation mechanisms and chemical properties of nanoparticles for developing drug delivery systems[29] and investigating catalysis mechanisms.[30] Finally, this method can find use in defect metrology for semiconductor fabrication and nanotechnology.[31]

Several straightforward avenues of improvement are available for our optical nanoparticle sizing method. Both the measurement accuracy and the dynamic range can be improved by replacing the air objective with an oil immersion objective featuring a larger numerical aperture and by minimizing background reflection[32] from the substrate. The scanning time can be reduced by using multiple confocal apertures.[33] Moreover, with larger training datasets one could make use of machine learning regression to further improve the sizing accuracy.[34]

The authors acknowledge Yichen Liu, Josh Akin, and Dishen Majithia for their help in the preparation of the manuscript and Jaehoon Choi for his assistance with the optical setup. S.S. and S.I.B. acknowledge the Strategic Research Initiative funding from the Grainger College of Engineering, University of Illinois at Urbana-Champaign.

DATA AVAILABILITY

The data that support the findings of this study are available from the corresponding author upon reasonable request.

REFERENCES

[1]N. Nath and A. Chilkoti, Anal. Chem. **76**, 5370 (2004).
[2]H. A. Atwater and A. Polman, Nat. Mater. **9**, 205 (2010).
[3]J. Kwon, J. Hong, Y.-S. Kim, D.-Y. Lee, K. Lee, S. Lee, and S. Park, Rev. Sci. Instrum. **74**, 4378 (2003).
[4]S. Hettler, M. Dries, P. Hermann, M. Obermair, D. Gerthsen, and M. Malac, Micron **96**, 38 (2017).
[5]M. P. Davidson and N. T. Sullivan, Proc. SPIE **3050**, 226 (1997).
[6]R. Attota, P. P. Kavuri, H. Kang, R. Kasica, and L. Chen, Appl. Phys. Lett. **105**, 163105 (2014).
[7]A. Barbara, F. Dubois, A. Ibanez, L. M. Eng, and P. Quémerais, J. Phys. Chem. C **118**, 17922 (2014).
[8]K. Braeckmans, K. Buyens, W. Bouquet, C. Vervaet, P. Joye, F. D. Vos, L. Plawinski, L. Doeuvre, E. Angles-Cano, N. N. Sanders, J. Demeester, and S. C. D. Smedt, Nano Lett. **10**, 4435 (2010).
[9]P. C. Ray, Chem. Rev. **110**, 5332 (2010).
[10]K. Lindfors, T. Kalkbrenner, P. Stoller, and V. Sandoghdar, Phys. Rev. Lett. **93**, 037401 (2004).
[11]A. Crut, P. Maioli, N. D. Fatti, and F. Vallée, Chem. Soc. Rev. **43**, 3921 (2014).
[12]T. Züchner, A. V. Failla, A. Hartschuh, and A. J. Meixner, J. Microsc. **229**, 337 (2008).
[13]B. T. Miles, A. B. Greenwood, B. R. Patton, and H. Gersen, ACS Photonics **3**, 343 (2016).
[14]Y. Colpin, A. Swan, A. V. Zvyagin, and T. Plakhotnik, Opt. Lett. **31**, 625 (2006).
[15]I. Pope, L. Payne, G. Zoriniants, E. Thomas, O. Williams, P. Watson, W. Langbein, and P. Borri, Nat. Nanotechnol. **9**, 940 (2014).
[16]W. W. Szymanski, A. Nagy, A. Czitrovszky, and P. Jani, Meas. Sci. Technol. **13**, 303 (2002).
[17]M.-H. Rim, E. Agocs, R. Dixson, P. Kavuri, A. E. Vladár, and R. K. Attota, J. Vac. Sci. Technol. B **38**, 050602 (2020).
[18]M. Hartmann, Acta Polym. **35**, 338 (1984).
[19]J. Zhu, S. K. Ozdemir, Y.-F. Xiao, L. Li, L. He, D.-R. Chen, and L. Yang, Nat. Photonics **4**, 46 (2010).
[20]R. G. Knollenberg, J. Aerosol Sci. **20**, 331 (1989).
[21]N. Li, T. D. Canady, Q. Huang, X. Wang, G. A. Fried, and B. T. Cunningham, Nat. Commun. **12**, 1744 (2021).
[22]N. Ohannesian, I. Misbah, S. H. Lin, and W.-C. Shih, Nat. Commun. **11**, 5805 (2020).
[23]J. Zhou, A. Panday, Y. Xu, X. Chen, L. Chen, C. Ji, and L. J. Guo, Phys. Rev. Lett. **120**, 253902 (2018).
[24]K. Lee, H.-D. Kim, K. Kim, Y. Kim, T. R. Hillman, B. Min, and Y. Park, Opt. Express **21**, 22453 (2013).
[25]S. I. Bogdanov, M. Y. Shalaginov, A. S. Lagutchev, C.-C. Chiang, D. Shah, A. S. Baburin, I. A. Ryzhikov, I. A. Rodionov, A. V. Kildishev, A. Boltasseva, and V. M. Shalaev, Nano Lett. **18**, 4837 (2018).
[26]S. I. Bogdanov, O. A. Makarova, A. S. Lagutchev, D. Shah, C.-C. Chiang, S. Saha, A. S. Baburin, I. A. Ryzhikov, I. A. Rodionov, A. V. Kildishev, A. Boltasseva, and V. M. Shalaev, arXiv:1902.05996 (2019).
[27]Y. Ding, Y. Dong, A. Bapat, J. D. Nowak, C. B. Carter, U. R. Kortshagen, and S. A. Campbell, IEEE Trans. Electron Devices **53**, 2525 (2006).
[28]J. J. Cully, J. L. Swett, K. Willick, J. Baugh, and J. A. Mol, Nanoscale **13**, 6513 (2021).
[29]M. Gaumet, A. Vargas, R. Gurny, and F. Delie, Eur. J. Pharm. Biopharm. **69**, 1 (2008).
[30]K. An and G. A. Somorjai, ChemCatChem **4**, 1512 (2012).
[31]R. Attota, R. G. Dixson, J. A. Kramar, J. E. Potzick, A. E. Vladar, B. Bunday, E. Novak, and A. Rudack, Proc. SPIE **7971**, 79710T (2011).
[32]A. Weigel, A. Sebesta, and P. Kukura, ACS Photonics **1**, 848 (2014).
[33]M. Liang, R. L. Stehr, and A. W. Krause, Opt. Lett. **22**, 751 (1997).
[34]T. Pu, J. Y. Ou, N. Papasimakis, and N. I. Zheludev, Appl. Phys. Lett. **116**, 131105 (2020).